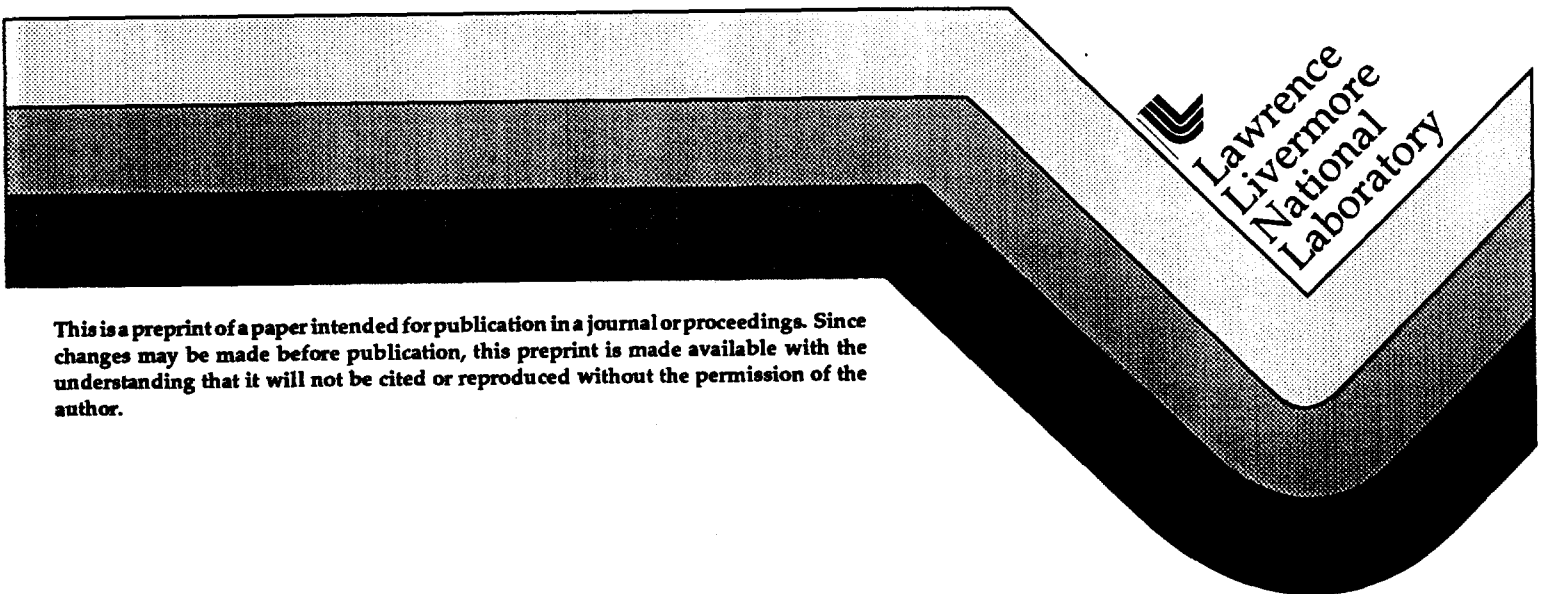# Review of Experiments and Calculations of the Compressible Richtmyer-Meshkov Instability from a Single-mode, Nonlinear Initial Perturbation

T. A. Peyser, S. D. Murray, P. L. Miller, D. R. Farley,
L. M. Logory, P. E. Stry, K. S. Budil, E. W. Burke

June 12, 1997

DISCLAIMER

Review of experiments and calculations of the compressible Richtmyer-Meshkov instability from a single-mode, nonlinear initial perturbation

T.A. Peyser[†] **S.D. Murray, P.L. Miller, D.R. Farley, L.M. Logory, P.E. Stry, K.S. Budil, E.W. Burke**
Lawrence Livermore National Laboratory
P. O. Box 808, L-22, Livermore, California, 94551, USA

Abstract: We review experiments and calculations of the compressible Richtmyer-Meshkov instability from a single-mode, nonlinear initial perturbation. These experiments were performed using the Nova laser. Measurements of the time-evolution of the mixing region were reported previously. We compared the experimental measurements with numerical simulations [1,2]. We found both experiment and simulation to be in good agreement with recent theories for the nonlinear evolution of the instability [3,4].

Experimental results beyond those previously presented provide additional support for the use of two phase flow models to describe the flow in the nonlinear regime. These experiments include measurement of the mixing region at additional times, including times earlier in the evolution of the instability than previously reported. We have also carried out experiments to examine the difference in the evolution of the instability from initial perturbations consisting of circular sawtooth grooves as well as rectilinear sawteeth. Our previous two-dimensional numerical simulations approximated the experimental linear grooves as circular grooves. We reasoned that the difference between the two cases would be small, based on scaling arguments, and limited to a very small region near the centerline. New experimental and numerical results confirm this. Finally, we discuss some additional issues in the derivation of the two-phase flow model used previously in describing the growth of the Richtmyer-Meshkov instability in the nonlinear phase relevant to other work presented at this meeting [5,6].

1. Review of the experiment

The experiments used a miniature beryllium shock tube mounted over a $700\,\mu$m diameter hole made at the center of the side of a $3\,$mm-long, $1.5\,$mm-diameter cylindrical gold Nova Hohlraum [7]. The shock tube was $2200\,\mu$m long, $700\,\mu$m in diameter with a $100\,\mu$m wall thickness. The working material of the shock tube consisted of a $500\,\mu$m-diameter, $300\,\mu$m-long section of a high-density ($1.22\,$g/cm^3) brominated polystyrene ablator and a $500\,\mu$m diameter, $1900\,\mu$m long low-density ($0.1\,$g/cm^3) carbon resorcinol foam payload. A schematic of the Hohlraum and the attached shock tube can be obtained elsewhere in these proceedings and in the literature [1,2,5,6]. Thermal x-ray radiation from the interior Hohlraum walls incident onto the exposed brominated polystyrene results in a rapid ablation of material and the generation of a strong shock ($85\,$Mbar) which travels down the shock tube towards the perturbed plastic-foam interface. A rectilinear sawtooth pattern was machined into the high density plastic with a high initial amplitude ($a_0 = 10\,\mu$m) relative to the dominant wavelength ($\lambda = 23\,\mu$m). The large amplitude-to-wavelength ($a_0/\lambda = 0.43$) initial perturbation was chosen so that the instability

---

[†]For more information - Email: peyser1@llnl.gov

would make an early transition into the nonlinear stage. The mixing region width was measured with high-speed gated x-ray framing camera diagnostics using radiography side-on to the shock tube cylinder axis [1,2,5,6].

2. Effect of Mach number on the spike and bubble amplitude

High-power laser-driven experiments make it possible to achieve extremely high Mach number shocks. At the time the shock is incident on the interface, the Mach number is greater than or equal to 20. This is important since experiments at high Mach number exhibit the effects of compressibility more strongly than low Mach number experiments.

The experiments were simulated using CALE, a two-dimensional arbitrary Lagrangian-Eulerian (ALE) hydrodynamics code [8]. In ALE-type codes, the mesh moves with the flow, giving added resolution in regions of high compression. Unlike purely Lagrangian codes, however, advection is allowed so as to avoid mesh tangling. For the simulations presented here, we use an initially rectilinear grid (unless otherwise noted) with 1 micron square resolution near the material boundary. The resolution decreases away from the boundary. Because the grid moves with the flow, however, high resolution of the mix region is maintained. The numerical simulations include the cylindrical region containing the plastic, the foam, the beryllium sleeve and a portion of the gold support ring. The effects of the laser drive are simulated by applying a temperature source to the edges of the plastic which extend into the hohlraum.

Previously, we found excellent agreement on the time evolution of the mixing region between the 2D CALE simulations and the measured results of the experiment. Fig. 1 shows the time evolution of the material interface during the growth of the instability. The calculations suggest, in contrast with incompressible or weakly compressible flows, that the Mach numbers of the present flows result in spike and bubble amplitudes of roughly comparable magnitudes [9]. As shown in Fig. 1a, the instability is well within the nonlinear regime by 4 ns (approximately 0.5 ns after the shock was incident on the interface). The similarity in the morphology of the spikes (heavy material) and bubbles (light material) is readily apparent at this time. The spikes and bubbles shapes and amplitudes in subsequent material plots at 5, 6 and 7 ns continue to appear highly symmetric as shown in Figs. 1b, 1c, and 1d.

A detailed comparison of the instability with a simulation of a smooth, unperturbed interface allows us to obtain quantitative estimates of the spike and bubble amplitudes as shown in Fig. 2a. The spike and bubble amplitudes in the perturbed calculation are determined by analysis of the material plots as in Fig. 1 above and comparison with the location of the unperturbed interface at the same time in the problem. We have followed the same procedure as in our earlier work and removed the effect of the axial target decompression to facilitate comparison between experiment and calculation on the one hand and nonlinear theory on the other hand [1,2]. Fig. 2b shows the growth of the overall mix region represented by the sum of the spike and bubble amplitudes (see below). The initial interface location for the unperturbed calculation was chosen to be $290 \, \mu m$, i.e., at the centerline of the $20 \, \mu m$ peak-to-valley sawtooth perturbation, so as to conserve the total mass of the high-density brominated polystyrene in the calculation. We assume that the presence of the instability does not significantly alter the overall hydrodynamic trajectory of the interface. This is consistent with estimates from the numerical simulations suggesting that the kinetic energy in the mix region is much less than 0.05 of the kinetic energy in the axial flow. We find that the spike and bubble amplitudes are roughly comparable (although not identical) for the duration of the calculation and the experiment.
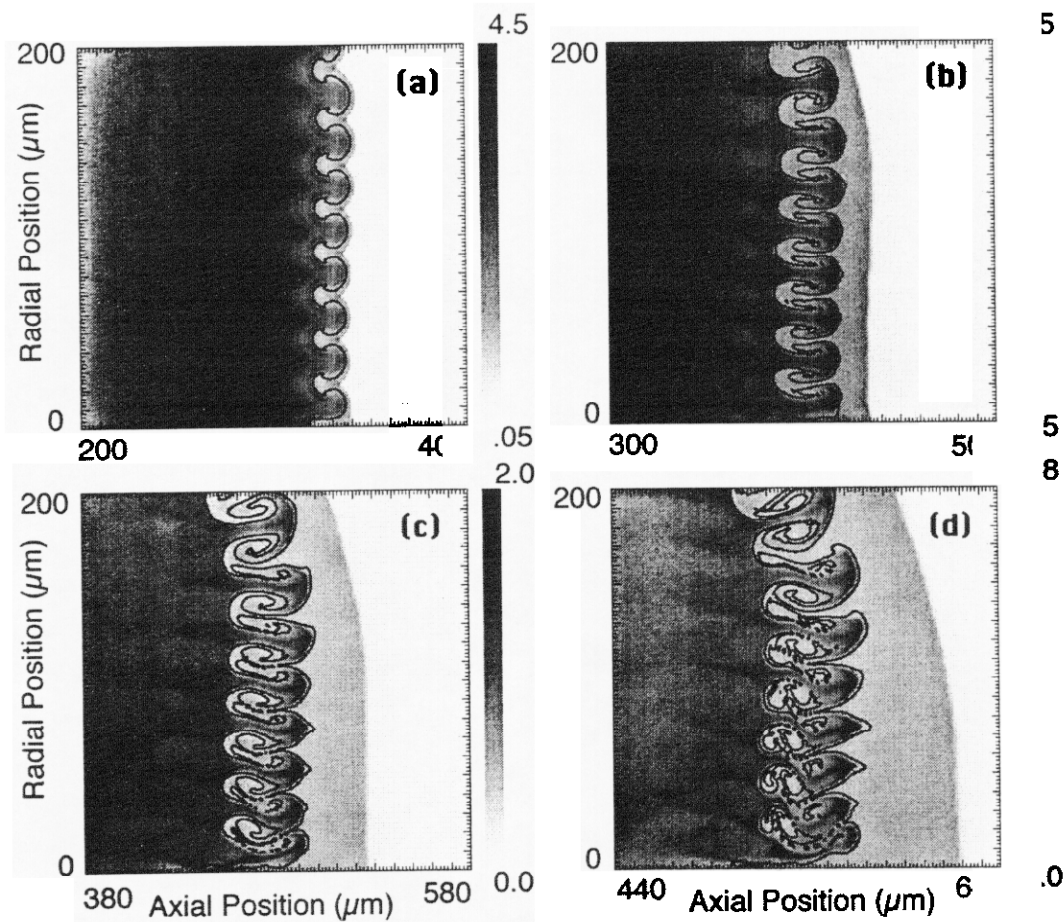
Figure 1. Density plots showing the time evolution of the material interface, from 2D CALE simulations, at (a) 4 ns, (b) 5 ns, (c) 6 ns, and (d) 7 ns
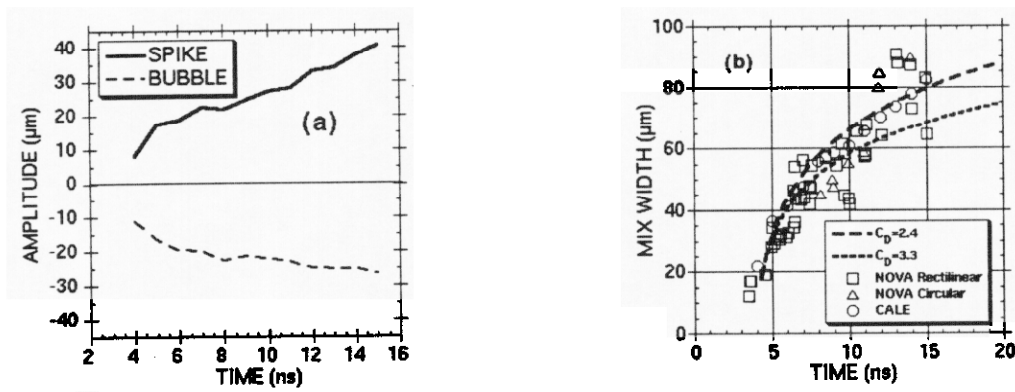

Figure 2. (a) Approximate spike and bubble amplitudes (corrected for axial target decompression), as a function of time, from comparison of perturbed and unperturbed 2D CALE simulations of the experiment; (b) Comparison of experimental data, 2D CALE simulations and results of a simple two-phase flow model for the nonlinear evolution of the instability using two values for the coefficient of drag

3. A simple two-phase flow model for nonlinear Richtmyer-Meshkov growth in the high Mach number regime

There are now numerous models for growth of the Richtmyer-Meshkov bubbles in the nonlinear regime which suggest that the evolution of the bubble velocity goes inversely with time for a single-mode perturbation. It follows accordingly that the bubble amplitudes in these models have a logarithmic time dependence [10-13]. As shown above, for conditions in the present experiment, the spike and bubble penetrations are roughly equal. The spikes are remarkably bubble-like in their appearance and time evolution, hence the total mix width for the single mode problem under these conditions can be approximated by a single, simple logarithmic time dependence [1,2].

We repeat here our derivation of a simple two-phase flow model with a clearer statement of the assumptions and the parameters in the model than provided earlier [1,2]. The equation of motion for a bubble of low density ρ_p displacing a heavier fluid of density ρ_c can be written as

$$V \left(\rho_c \frac{\Delta_A}{2} + \rho_p \right) \frac{dU}{dt} = F_a - A\, C_d\, \rho_c\, U^2 \tag{1}$$

where V is the volume of the bubble, $\Delta_A/2$ is the added mass coefficient, A is the frontal area (A $= \pi\, d^2/4$ for bubble of diameter d) and C_d is the coefficient of drag. Numerous experiments on bubble rise beginning with the work of Davies et al. in the early 1950s have shown that the bubble front retains its spherical character during its rise [14]. This is consistent with more recent compilations of bubble geometry at high Reynolds numbers applicable to this problem [15]. Since we are invoking nonlinear theory only when the amplitude and wavelength are comparable, it is permissible from the assumption of sphericity as well as from general dimensional analysis to treat the ratio of area to volume in Eq. 1 as a characteristic scalelength given by the wavelength λ of the single mode perturbation. In the high velocity limit, the added mass coefficient $\Delta_A/2$ is equal to one. Finally we assume further that there are no additional forces (gravity, pressure gradient terms etc.) acting on the system. Eq. 1 then becomes

$$\frac{dU}{dt} = -\frac{C_d}{\lambda} \left(\frac{\rho_c}{\rho_c + \rho_p} \right) U^2 \tag{2}$$

Eq. 2 can be rearranged and integrated to give the following expression for the bubble velocity

$$U = \frac{U_0}{1 + U_0\, m\, t} \tag{3}$$

where

$$m = \frac{C_d}{\lambda} \left(\frac{\rho_c}{\rho_c + \rho_p} \right) \tag{4}$$

Finally, a further integration of Eq. 3 gives

$$a = a_0 + \frac{1}{m} \ln[1 + m\, U_0\, (t - t_0)] \tag{5}$$

where a_0 is the initial nonlinear amplitude, m is given by Eq. 5 above and depends on the coefficient of drag, the densities of the material and the wavelength of the perturbation, U_0 is the initial relative velocity of the bubbles (compared to the nominal interface location) after the passage of the shock and is the time at which the nonlinear phase of the instability

begins. Given the similarity between spike and bubble amplitude growth in the high Mach numbers of the present problem, Eq. 5 can be rewritten as an equation for the total mix width evolution w where w_0 is equal to two times the instantaneous nonlinear amplitude and U_0 is the instantaneous spike (or bubble) velocity relative to the nominal interface at the time of onset of nonlinearity.

$$w = w_0 + \frac{2}{m}\ln[1 + m\,U_0\,(t - t_0)] \tag{6}$$

Since we do not know the values of the initial nonlinear amplitudes, relative velocities or time of onset of nonlinearity either a priori or directly from the experimental data, we make use of the 2D numerical simulation to obtain estimates of these quantities. An examination of the calculations suggests that the instability begins to exhibit nonlinearity at approximately 3.8 ns to 4.3 ns. Fig. 3 shows the density and velocity plots at 3.8 ns from the 2D CALE simulations. At this time, we find from the simulations that the total mix width $w_0 = 18\,\mu m$ and the velocity
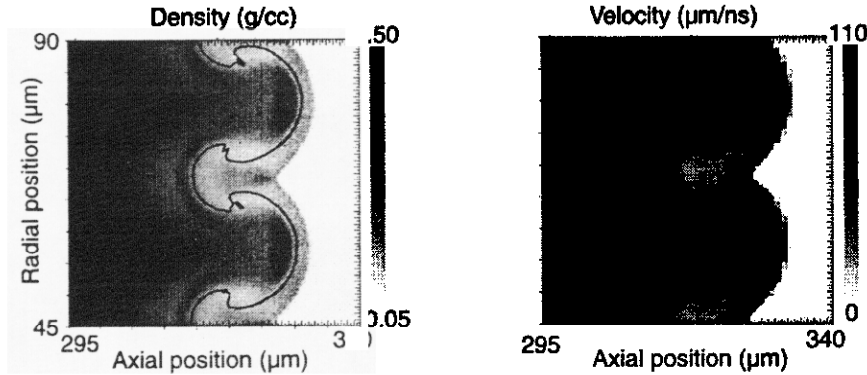

Figure 3. Density and velocity plots at 3.8 ns showing onset of nonlinear amplitudes from 2D CALE simulation

of the spike and bubble relative to the nominal interface $U_0 = 14\,\mu m\,/ns$. A least squares fit of the data shows further that the behavior of the measured mixing region admits a logarithmic time dependence with $m = 0.096\,\mu m^{-1}$. Assuming densities in Eq. 4 of $\rho_c = 0.4\,g/cm^3$ and $\rho_p = 1.6\,g/cm^3$ consistent with the numerical simulation, we find a value for the apparent coefficient of drag $C_d \approx 2.8 \pm 0.4$ where the uncertainty is due to the scatter in the data as well as the simplifying assumption used in the model. Predictions from the nonlinear theory for two values of the coefficient of drag are shown above in Fig. 2b. Interestingly, the coefficient of drag thus inferred from this experiment is consistent with published values for an air bubble in water at high Reynolds numbers [15].

4. Additional experimental data on the nonlinear mix width

Measurements from additional experiments carried out subsequent to the results reported previously are shown in Fig. 2b above. As with the previous results, the total mix width is inferred from a detailed analysis of the 5 − 95% transmission of x-rays across the nominal mix region. The experimental data (squares) are in good agreement with both the numerical simulation (circles) and Eq. 6 above using the quoted parameters. These data points were all obtained with initial perturbations that were rectilinear in nature as shown in a high-resolution scanning electron microscope image in Fig. 4a. We have also plotted the measured mix width from experiments in which the initial perturbations were circular in nature as shown in Fig. 4b. There
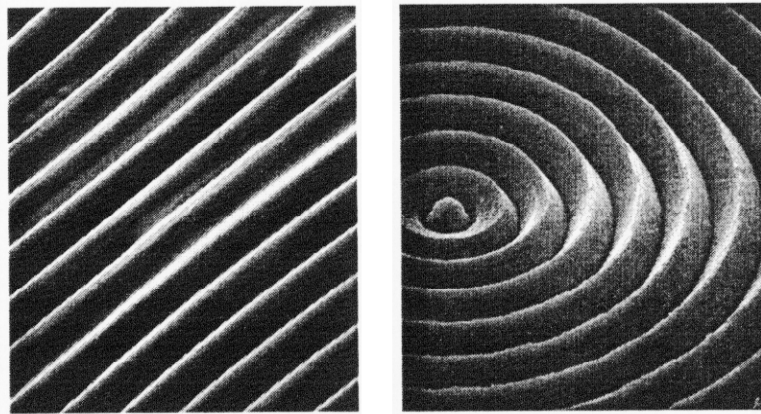
Figure 4. High-resolution scanning electron microscope image of (a) the original rectilinear sawtooth perturbations and (b) the curvilinear perturbations

appears to be little difference between the two perturbation types which affirms the use of a two-dimensional axisymmetric code to simulate the instability growth from the non-axisymmetric perturbations used in the experiment. We have also found little difference in the growth of the mix region between numerical simulations having cylindrical and Cartesian geometries. This is not surprising from simple dimensional considerations since the radius of curvature in the calculations is large compared with the amplitude and wavelength of the perturbation.

References

[1] T.A. Peyser *et al.*, in: *Proceedings of the Fifth IWCTM*, 257 (1996).

[2] P.L. Miller *et al.*, in: *Proceedings of the Twentieth ISSW*, 581 (1996).

[3] T. A. Peyser, *et al.*, *Phys. Rev. Lett.* 75, 2332 (1995).

[4] U. Alon *et al.*, *Phys. Rev. Lett.* **72**, 2867 (1994); J. Hecht *et al.*, *Phys. Fluids* **6**, 4019 (1994).

[5] D.R. Farley *et al.*, these proceedings.

[6] L.M. Logory *et al.*, these proceedings.

[7] E.M. Campbell, *Lasers and Particle Beams* **9**, 209-231 (1991).

[8] R.T. Barton, in: *Numerical Astrophysics*, 482 (1985).

[9] D. Shvarts, D. Oran, personal communication (1997).

[10] J. Hecht, U. Alon, D. Shvarts, *Phys. Fluids* **6**, 4019-4030 (1994).

[11] S.W. Haan, *Phys. Rev.* A **39**, 5812-5825 (1989).

[12] J.W. Jacobs and J.M. Shelley, *Phys. Fluids* **8**, 405 (1996).

[13] Q. Zhang and S. Sohn, *Phys. Fluids* **9**, 1106 (1997).

[14] R.M. Davies and G. Taylor, *Proc. Roy. Soc of London* A **200**, 375 (1950).

[15] R. Clift, J.R. Grace and M.E. Weber, *Bubbles, Drops and Particles*, Academic Press, NY (1978).